

1 Site effect classification based on microtremor data 2 analysis using Concentration-area fractal model

3
4 **Ahmad Adib^{1*}, Peyman Afzal^{1, 2}, Kobra Heydarzadeh³**

5 [1]{Department of Mining Engineering, Faculty of Engineering, South Tehran Branch, Islamic Azad
6 University, Tehran, Iran}

7 [2]{Camborne School of Mines, University of Exeter, Penryn, UK}

8 [3]{Zamin Kav Environmental & Geology Research Center, Tehran, Iran}

9 *Correspondence to: Ahmad Adib (adib@azad.ac.ir)

10 11 **Abstract**

12 The aim of this study is to classify the site effect using concentration-area (C-A) fractal model
13 in Meybod city, Central Iran, based on microtremor data analysis. Log-log plots of the
14 frequency, amplification and vulnerability index (k-g) indicate a multifractal nature for the
15 parameters in the area. The results obtained from the C-A fractal modeling reveal that proper
16 soil types are located around the central city. The results derived via the fractal modeling were
17 utilized to improve the Nogoshi's classification results in the Meybod city. The resulted
18 categories are: (1) hard soil and weak rock with frequency of 6.2 to 8 Hz, (2) stiff soil with
19 frequency of about 4.9 to 6.2 Hz, (3) moderately soft soil with the frequency of 2.4 to 4.9 Hz,
20 and (4) soft soil with the frequency lower than 2.4 Hz.

21 **Keywords:** Site effect classification, Concentration-area fractal model, Microtremor,
22 Frequency, Meybod city, Iran

23 24 **1 Introduction**

25 Site effect caused by an earthquake may vary significantly in a short distance., Seismic waves
26 trapping phenomenon leads to amplify vibrations amplitudes that may increase hazards in
27 sites with soft soil or topographic undulations. Theoretical analysis and observational data
28 have illustrated that each site has a specific resonance frequency at which ground motion gets
29 amplified (Bard, 2000; Mukhopadhyay and Bormann, 2004).

1 Microtremor data analysis is applied in the recognition of the soil layers, prediction of shear-
2 wave velocity of the ground, and evaluation of the predominant period of the soil during
3 earthquake events. It has been proved that measurement and analysis of microtremor data is
4 an efficient and low-cost method of seismic hazard micro zonation (Kanai and Tanaka, 1954;
5 AIJ, 1993; Mukhopadhyay and Bormann, 2004; Beroya et al., 2009). Microtremors are weak
6 ground motions with amplitude between 1 and 10 μm which always exist and are mostly
7 generated by natural processes. Since these motions change the site effects and these changes
8 are representative of the soil characteristics, microtremors analysis is used to obtain
9 information about soil vibration properties of sites (Kamalian et al., 2008).

10 Some scientists believe that the microtremors are mostly formed by Love and Rayleigh waves
11 (Akamatu, 1961). However, they could be composed of Longitudinal and Rayleigh waves
12 (e.g. Douze et al., 1964). Allam (1969) proposed that microtremors could be composed of
13 body and/or surface waves and thus, it is possible that they are originated from any wave.

14 Microtremors are also applied to calculate the amplifications of horizontal movements in the
15 free surface during earthquake events (Nakamura, 1989). Fundamentally, the method
16 expressed the spectral amplification of a surface layer which could be obtained by evaluation
17 of the horizontal to vertical spectral ratio of recorded microtremors. The amplification factor
18 was resulted by several refracted waves in effect of their incidence into layer boundary. Thus,
19 associated Rayleigh wave of microtremor would be a noise and is removed during H/V
20 process. Moreover, H/V ratios of simultaneously measured records on ground surface and
21 bedrock represented constant maximum acceleration ratio. Since every station has different
22 characteristics, the records of one earthquake in various sites will be different. In soft soil
23 location underlying a hard rock, H/V spectral ratio illustrates a clear peak. These peaks are
24 spatially and temporally stable and could be considered as a fundamental (resonance)
25 frequency of the site (Duval et al., 1994; Duval, 1996). This method is used by many
26 scientists in order to identify small scale seismic risks and prepare detailed data for urban
27 seismic microzonation. Konno and Ohmachi (1998) carried out a complete study about
28 Nakamura's approximation and developed the matter to investigate multi-layered systems
29 which is known as HVSR method. It is obtained from numerical studies of horizontal
30 geological deposits that if there would be large impedance differences between deposits and
31 bedrock, local fundamental frequency could be well presented by HVSR method. However,
32 comparison of HVSR peaks with standard spectral ratio shows that the actual site

1 amplification cannot be estimated from the amplitudes of HVSR peaks (Bard, 1998; Gosar et
2 al., 2008; Sesame, 2004).

3 Identification of ground types is a main issue in the seismic geotechnical studies as well as
4 site selection. There are many site effect classifications based on dynamical ground
5 characteristics such as frequency, period, alluvial thickness, and shear wave velocity. Nogoshi
6 and Igarashi (1971) proposed one of the common classifications of site effects (Table 2).

7 Additionally, Komak Panah et al.(2002) presented a classification based on HVSR method in
8 the eastern and central Iran. Both used fundamental frequency as a main factor (Tables 1 and 2).

9 Table 1. Site effect classification of Komak Panah et al. (2002)

Geological Condition	V_s^{30} (m/s)	Predominant Frequency (Hz)	Soil Description	Class No.
Thick soft clay or silty sandy clay mostly alluvial plain	<350	<2.5	soft soil	I
Interbedded of fine and coarse material, alluvium terraces with weak cementation	350- 550	2.5-5	moderately soft soil	IIa
Thick old alluvium terraces or colluviums soils with medium to good cementation	550- 750	5-7.5	stiff soil	IIb
Well cemented and compacted soil, old quaternary outcrop	>750	>7.5	hard soil, weak rock	III

10

11 Table 2. Site effect classification of Nogoshi & Igarashi (1970)

Describision	Frequency (Hz)	Type
Stiff rock composed of gravel, sand and other soils mainly consisting of tertiary or older layers	7-10	I
Sandy gravel, stiff sandy clay, loam or sandy alluvial deposits whose depths are 5 m or greater	4.5-7	II
Standard grounds other than type I, II or IV	2-4.5	III
Soft alluvium-delta lands and pit whose depth is 20m or greater. Reclaimed land from swamps or muddy shoal where the ground depth is 2m or greater and less than 20 years have passed since the reclamation.	0/1-2	IV

1 Euclidean geometry recognizes geometrical shapes with an integer dimension; 1D, 2D, and
2 3D. However, there are many other shapes or spatial objects whose dimensions cannot be
3 mathematically explained by integers, but by real numbers or fractions. These spatial objects
4 are called fractals. In abstract form, fractals describe complexity in data distribution by
5 estimation of their fractal dimensions. Different geophysical and geochemical processes can
6 be described based on differences in fractal dimensions obtained from analysis of relevant
7 geophysical data. Fractal models which established by Mandelbrot (1983) were applied to
8 objects that were too irregular to be described by ordinary Euclidean geometry (Davis, J.C.,
9 2002; Evertz and Mandelbrot, 1992). Fractal theory has been practical to geophysical and
10 geochemical exploration since late 1980s (e.g., Agterberg et al., 1996; Afzal et al., 2010;
11 2011; 2012; 2013; Cheng et al., 1994; Daneshvar et al., 2012; Sim et al., 1999; Turcotte,
12 1986). Cheng et al. (1994) proposed a concentration-area(C-A) fractal model based on the
13 relationship of elemental distributions and occupied areas. This idea and premise provided a
14 scientific tool to demonstrate that an empirical relationship between C-A exists in the
15 geophysical and geochemical data (Afzal et al., 2010; 2012; Cheng et al., 1994; Cheng, 1999;
16 Goncalves et al., 2001; Sim et al., 1999). Cheng et al. (1994) showed that there are various
17 parameters which have a key role in spatial distributions of most of the elements for a given
18 geological-geochemical environment.

19 In this paper, fundamental frequency, amplification and ground vulnerability index (K-g
20 value) data of Meybod city (Central Iran) are separated by C-A fractal model and Nogoshi's
21 classification. Subsequently, results obtained by the both methods are compared.

22

23 **2 Case study characteristics**

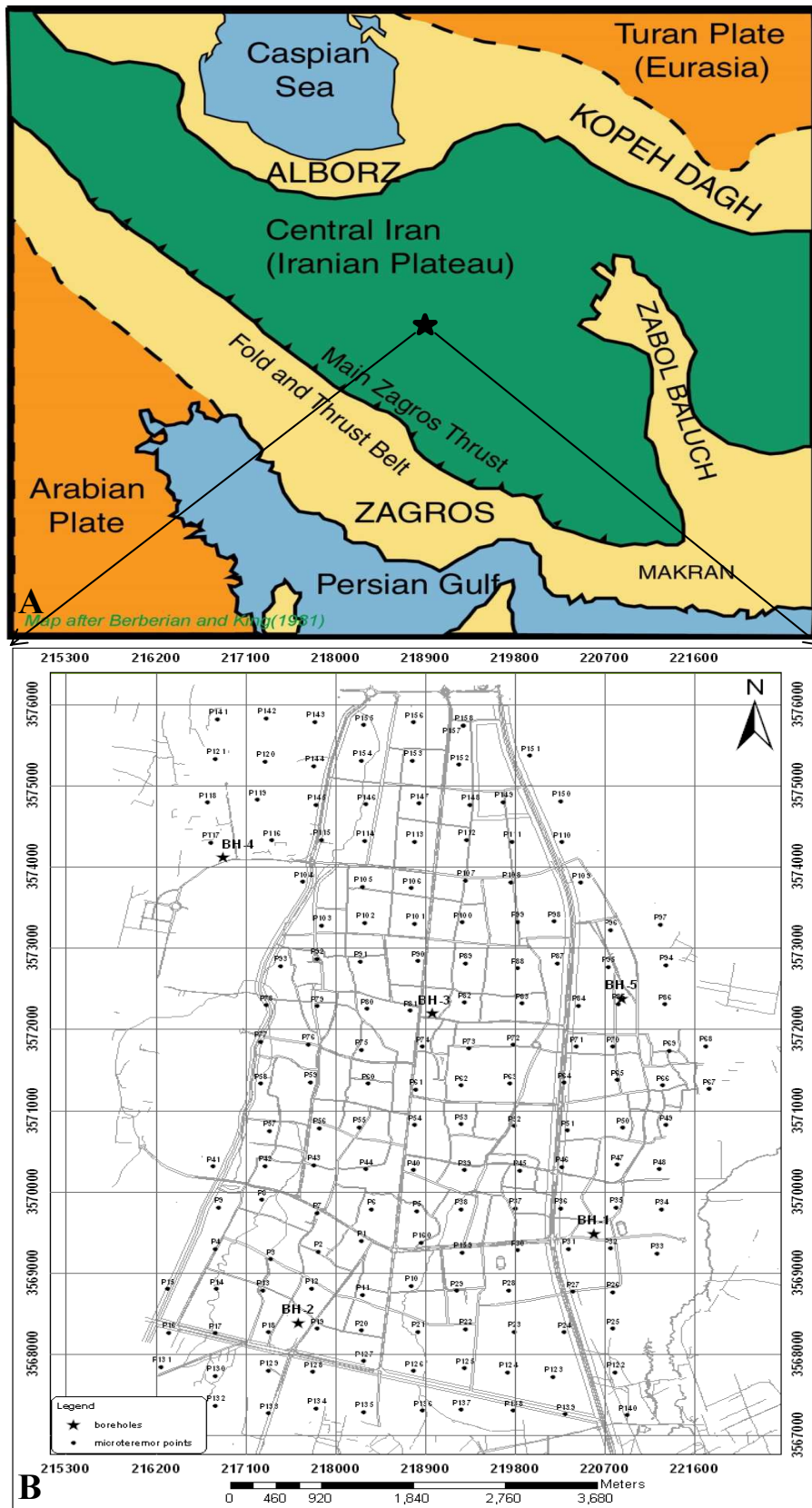
24 Meybod city is located in the Yazd province, central Iran (Fig. 1), with Quaternary sediments
25 as the major geological units (Fig. 2). Major types of the sediments are clay and silty-clay in
26 the area. Additionally, Sandy-clay units occurred in the NE part of the city with 2 m thickness
27 and deep as 30-32 m.

28

29

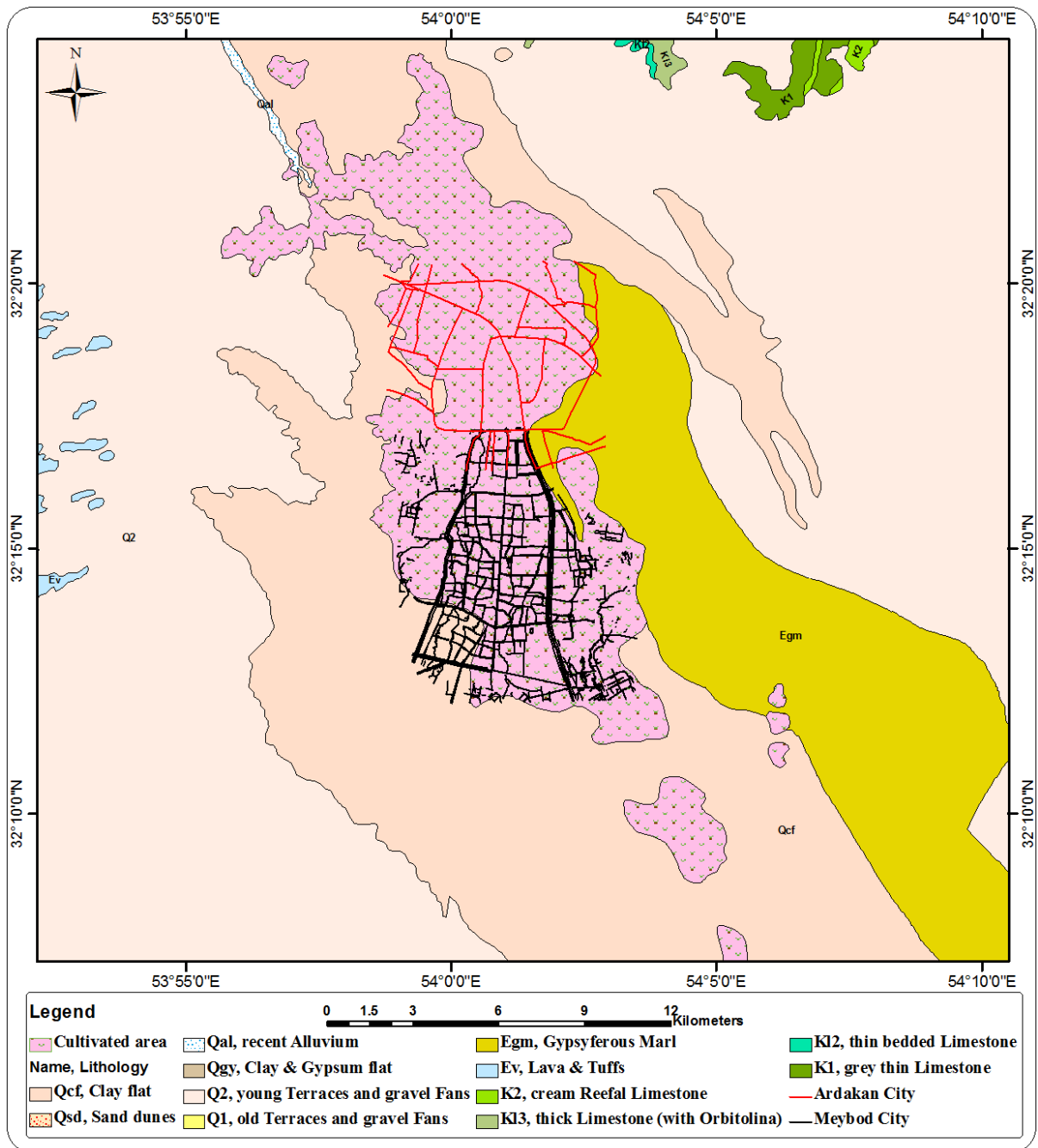
30

31



1
2
3
4
5
6
7
8
9
10
11
12
13
14
15
16
17
18
19
20
21
22
23
24

25 Figure 1. A) The location of the study area (black star) in Iran; B) The microtremor recording
26 points and boreholes map.

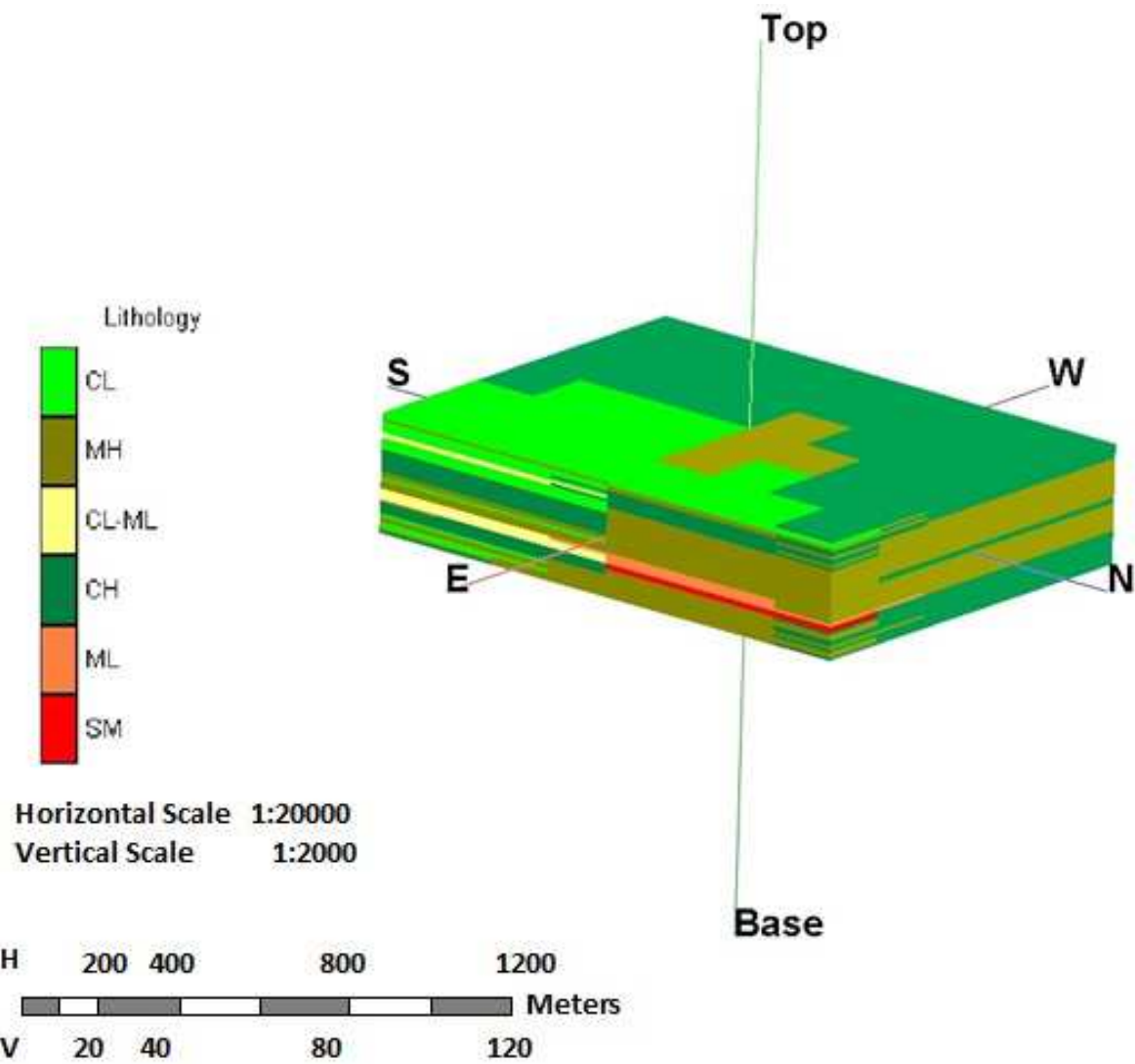


1

2 Figure 2. Geological map of Meybod area. According to the map, the major units around the city are
 3 Quaternary deposits including cultivated land, Clay flat and young terraces and fans. The only other unit that is
 4 close to the city is Eocene gypsiferous Marls (Egm).

5

6 Based on the geotechnical studies of the region, dominant soil type is composed of clay and
 7 silt with high plasticity (Fig 3). Additionally, there is not any major variation in the
 8 composition of sediment in the area, except for some variation of clay and silt contents in the
 9 eastern part (based on borehole data) (Fig 3).



1

2 Figure 3. 3D model of soil deposits of Meybod city, Iran. Dominant soil type is composed of
 3 clay and silt with high plasticity. The major variation is located in the eastern part of the city
 4 (CL: inorganic Clay of low plasticity or lean Clay; MH: inorganic Silt of high plasticity; CL-
 5 ML: inorganic Clay and inorganic Silt of low plasticity; CH: inorganic Clay of high plasticity;
 6 ML: inorganic Silt of low plasticity; SM: silty Sand).

7 From the down hole data which are collected from 5 boreholes, the variations of P and S
 8 velocity (m/s) were calculated (table 3). Shear wave velocity is between 560 and 725 m/s in
 9 the depth of 42 m. the depth of seismic bedrock varies from 52 to 90 m which are calculated
 10 based on the velocity. This result shows that there are differences in soil hardness values
 11 within the area.

12

13

1 Table3. Velocity of seismic waves (m/s) in the Meybod city

Borehole	B.H1		B.H2		B.H3		B.H4		B.H5	
Depth(m)	Vs	Vp	Vs	Vp	Vs	Vp	Vs	Vp	Vs	Vp
1.0	243	567	308	659	217	477	157	353	352	782
2.0	329	743	356	759	283	615	225	501	415	905
4.0	441	961	440	936	360	784	311	685	520	1100
6.0	505	1081	464	997	407	882	377	820	548	1155
8.0	532	1132	487	1045	451	968	405	881	561	1177
10.0	521	1121	505	1080	473	1015	428	927	568	1192
12.0	517	1121	523	1114	503	1070	449	969	592	1231
14.0	505	1108	537	1141	525	1111	476	1019	612	1262
16.0	490	1086	551	1164	525	1118	494	1053	625	1286
18.0	493	1093	564	1188	528	1130	507	1078	628	1292
20.0	497	1097	573	1207	535	1142	506	1081	643	1316
22.0	503	1108	585	1228	550	1169	512	1094	651	1330
24.0	509	1119	595	1244	562	1190	522	1113	662	1345
26.0	518	1135	602	1256	575	1211	525	1121	672	1361
28.0	526	1149	605	1263	585	1227	532	1134	683	1377
30.0	534	1163	609	1271	592	1240	543	1152	692	1390
32.0	539	1169	616	1283	601	1254	552	1168	700	1403
34.0	541	1172	624	1295	603	1259	562	1184	703	1411
36.0	545	1176	631	1306	610	1269	571	1197	708	1419
38.0	551	1185	637	1315	617	1280	577	1208	714	1428
40.0	555	1192	644	1325	623	1291	581	1215	719	1436
42.0	559	1199	650	1335	629	1301	588	1226	725	1444
Vs30 (m/s)	473		509		460		407		579	
seismic bed rock depth(m)	70		90		80		80		52	

1 **3 Methodology**

2 Measured microtremor data were analyzed by Nakamura technique (HVSR: Nakamura, 1989)
3 and using SESAME software, based on Fast Fourier Transform (FFT). The results were
4 mapped by Inverse Distance Squared (IDS) method using Rockworks TM v.15 software
5 package. The results are fundamental frequency, amplification and ground vulnerability index
6 (K-g value); K-g value has obtained by Equation (1): (Nakamura, 1996):

$$7 \quad Kg = (A_0)^2 / F_0 \quad (1)$$

8 where F0 and A0 are predominant frequency and its amplification factor, and K-g is an index
9 to indicate deformation easiness of measured points which is expected to be useful to detect
10 weak points of the ground (Nakamura, 1997).

11 For instance, K-g values obtained in San Francisco Bay Area after the 1989 Loma-Prieta
12 Earthquake are bigger than 20 at the sites where grounds were deformed significantly and
13 very small at the sites with no damage (Nakamura et al., 1990). However, Comparison
14 between K-g values obtained before the earthquake in 1994 and the damage degrees show that
15 places with large K-g values correspond to the sites with big damage. This suggests K-g
16 values representing the vulnerability precisely (Nakamura, 1997).

17 **3.1 Concentration–area fractal model**

18 Cheng et al. (1994) proposed concentration–area (C–A) model, which may be used to define
19 the geophysical background and anomalies. The model is in the following general form:

$$20 \quad A(\rho \leq v) \propto \rho^{-a1}; A(\rho \geq v) \propto \rho^{-a2} \quad (2)$$

21 where $A(\rho)$ is the area with concentration values (frequency, amplification and K-g in this
22 study) greater than the contour value ρ ; v is the threshold; and $a1$ and $a2$ are characteristic
23 exponents.

24 The frequency size distributions for islands, earthquakes, fragments, ore deposits and oil
25 fields often confirm the Equation (2) (Daneshvar Saein et al., 2012). The two approaches
26 which were used to calculate $A(\rho)$ by Cheng et al. (1994) were: (1) The $A(\rho)$ is the area
27 enclosed by contour level ρ on a variables' contour map resulting from interpolation of the
28 original data using a weighted moving average method, and (2) The $A(\rho)$ are the values that
29 are obtained by box-counting of original regional variables' values. The breaks between

1 straight-line segments on C-A log-log plot and the corresponding values of ρ have been used
2 as thresholds to separate geophysical values into various components, showing different
3 causal factors, such as lithological and mineralogical differences, geochemical and
4 geophysical processes and mineralizing events (Lima et al., 2003; Afzal et al., 2010; 2012;
5 Heidari et al., 2013).

6 Fractal models are often used to describe self-similar geometries, while multifractal models
7 have been utilized to quantify patterns; same as geophysical data defined on sets which
8 themselves can be fractals. Extension from geometry to field has considerably increased the
9 applicability of fractal/multifractal modeling (Cheng, 2007). Multifractal theory could be
10 interpreted as a theoretical framework that explains the power-law relationships between areas
11 enclosing concentrations below a given threshold value and the actual concentrations itself.
12 To demonstrate and prove that data distribution has a multifractal nature requires a rather
13 extensive computation (Halsey et al., 1986; Evertsz and Mandelbrot, 1992). This method has
14 several limitations such as accuracy problems, especially when the boundary effects on
15 irregular geometrical data sets are involved (Agterberg et al., 1996; Goncalves, 2001; Cheng,
16 2007; Xie et al., 2010).

17 The C-A model seems to be equally applicable as well to all cases, which is probably rooted
18 in the fact that geophysical distributions mostly satisfy the properties of a multifractal
19 function. Some evidences prove that geophysical data distributions are fractal in nature and
20 behavior (e.g., Bolviken et al., 1992, Turcotte, 1997, Gettings, 2005, Afzal et al., 2012, and
21 Daneshvar Saein et al. 2012).

22 This idea may provide and help the development of an alternative interpretation validation as
23 well as useful methods to be applied to geophysical distributions analysis (Afzal, 2012).
24 Various log-log plots between a geometrical character such as area, perimeter or volume and a
25 geophysical quality parameter like geoelectrical data in fractal methods are appropriate for
26 distinguishing geological recognition and populations' classification in geophysical data
27 because threshold values can be identified and delineated as breakpoints in those plots
28 (Daneshvar Saein et al., 2012).

29

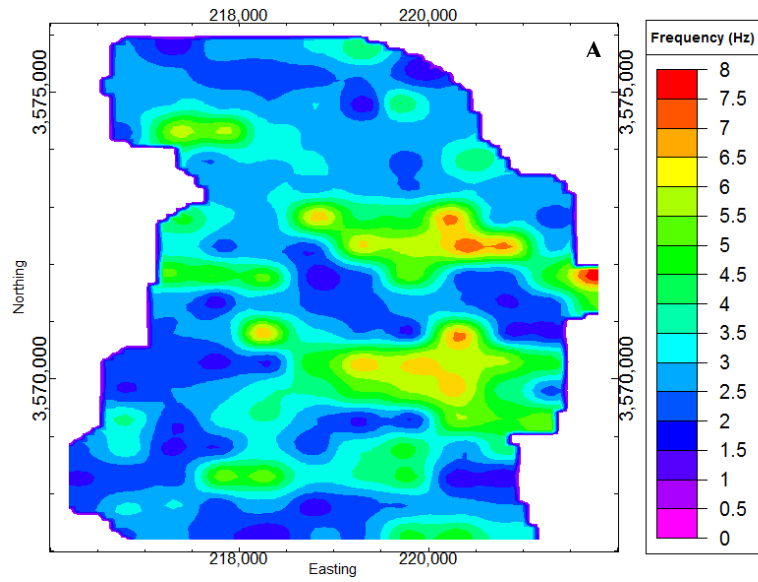
1 **4 Application of C-A model**

2 Microtremor data are measured at 160 point in the study area (Fig. 1) using three channeled
3 seismometer device (SL07, SARA Company, Italy). It has natural frequency of 2 Hz and
4 natural attenuation of 0.7. This device has a three channeled digitizer of 24 bit, a central
5 process unit (CPU) to save records and a GPS receiver. The data were recorded by sampling
6 frequency of 200 Hz and the average recording time of 12 minutes at each station. At first, a
7 mesh was overlapped on the city map to determine the recording points. Then, recording on
8 every point was regularly performed. When any of recording points was not appropriate for
9 recording (e.g. because of existence of tall buildings), the point location was slightly shifted
10 to achieve a clear data. Moreover, if any point was approximate to a heavy traffic street, the
11 data were recorded at midnight. During recording process, the device was located on a leveled
12 ground and was balanced. Usually, 10 min is required for any microtremor recording to
13 record the minimum 1 Hz frequency (WP12 Sesame project, 2004).

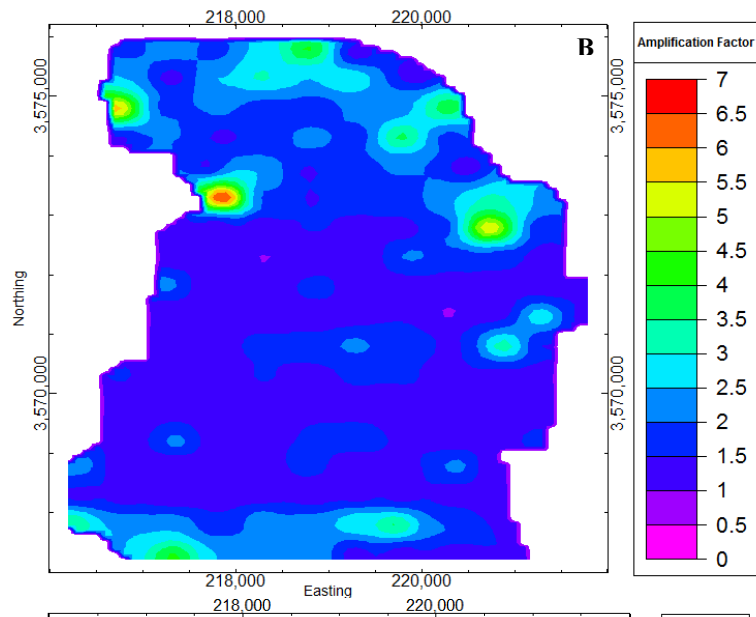
14 The obtained frequencies, amplifications and $K-g$ values are illustrated as contour maps
15 applying IDS interpolation method (Fig. 4). The areas with different frequencies can be
16 visually distinguished in the map. The studied area was gridded by 20×20 m cells. The
17 evaluated values in cells were sorted out based on decreasing grades, and cumulative areas
18 were calculated for grades. Eventually, log-log graphs were plotted to separate the different
19 populations.

20 Distributions of the fundamental frequency, amplification and $K-g$ data are multimodal which
21 their mean values are 3.24 Hz, 2.14 and 2.91, respectively (Fig. 5). The separated populations
22 are clear in their histograms and also, high amounts of the parameters are lower than their
23 means. Moreover, their median could be assumed for their threshold values because their
24 distributions are not normal. The medians are 2.6 Hz, 1.6 and 1.1 for frequency, amplification
25 and $K-g$ respectively. Moreover, the median values of these parameters are low for their
26 threshold values. Variograms and anisotropic ellipsoids of the parameters were calculated to
27 estimate data influence range of any point in order of plotting IDS maps (Fig. 6). These
28 ellipsoids make the results estimated more accurate and we can determine the direction of the
29 results variations. Based on the variograms and ellipsoids of the parameters, their major
30 ranges have a W-E trend. It could be represented by the direction of soil variations that
31 become more intense from west to the east of the area (Fig. 3).

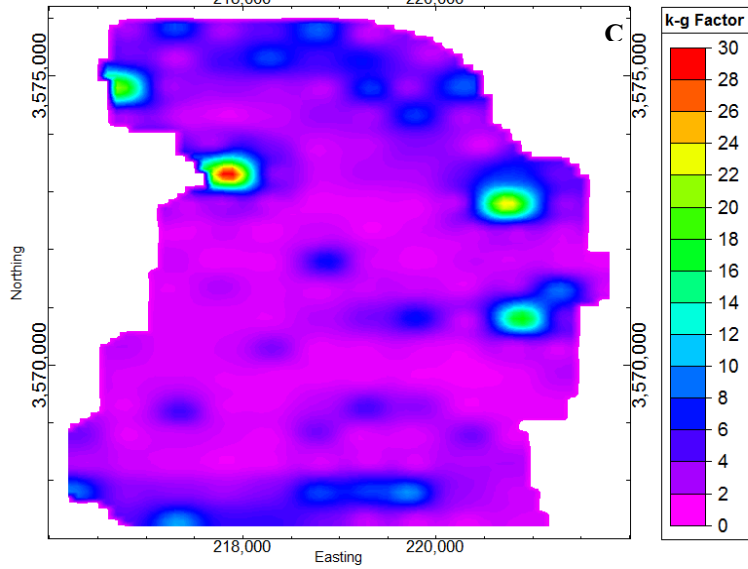
1



2



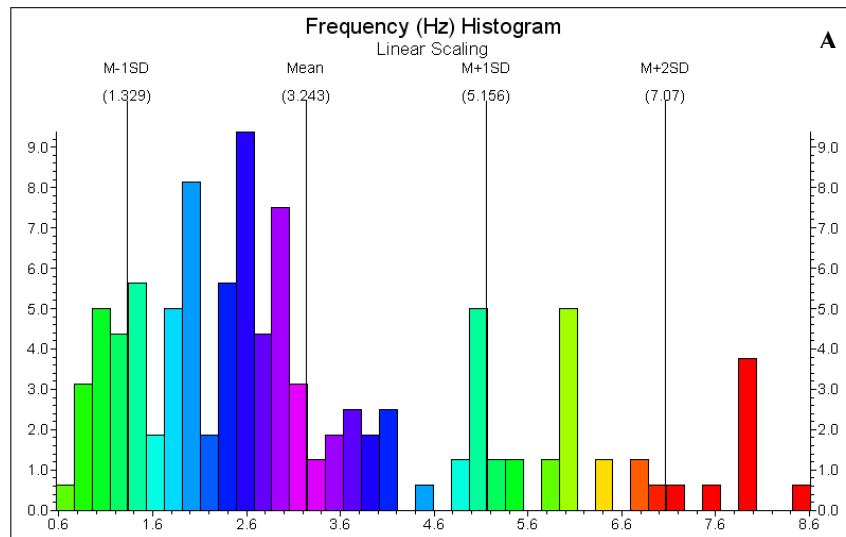
3



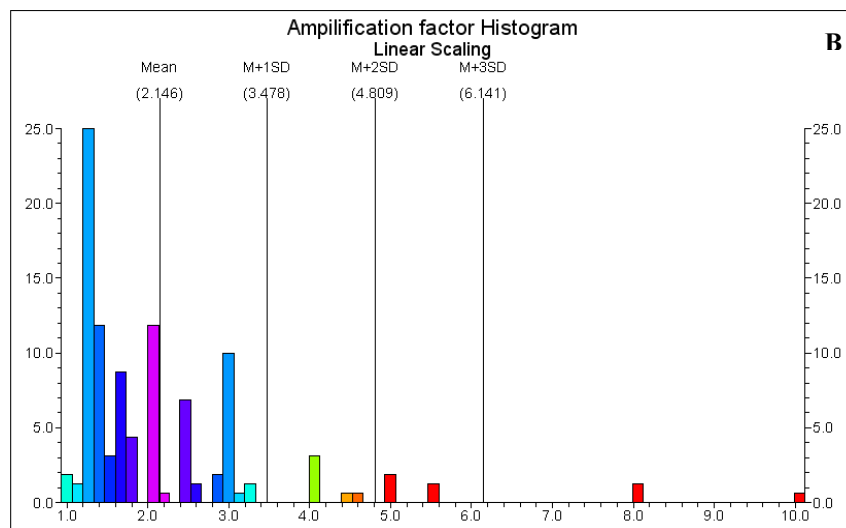
4

Figure 4. Data distribution maps in the Meybod city: A) frequency; B) amplification; C) K-g value.

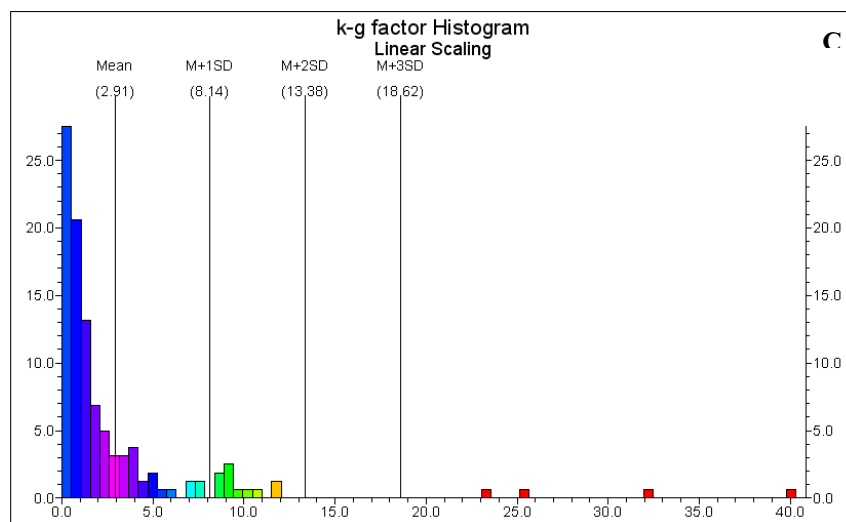
1



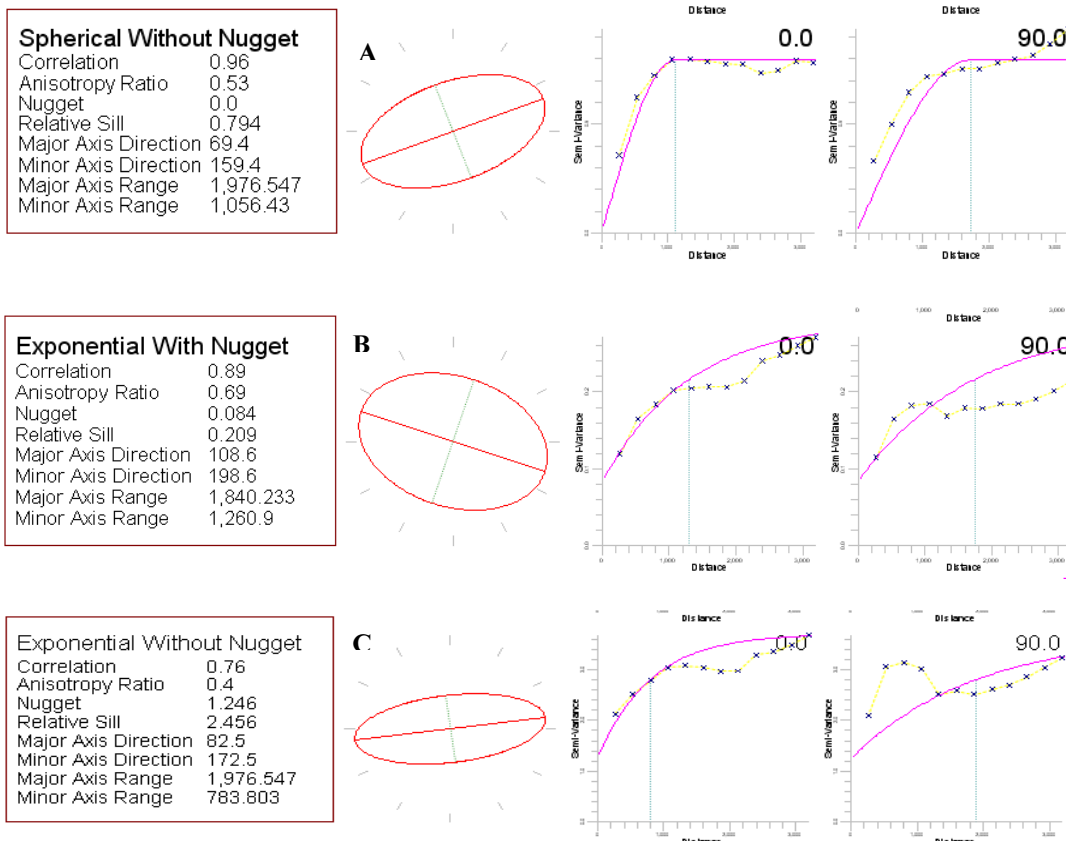
2



3



4 Figure 5. Data histograms show multimodality of the factors. A) Frequency, B) amplification,
5 C) K-g value



1

2

3

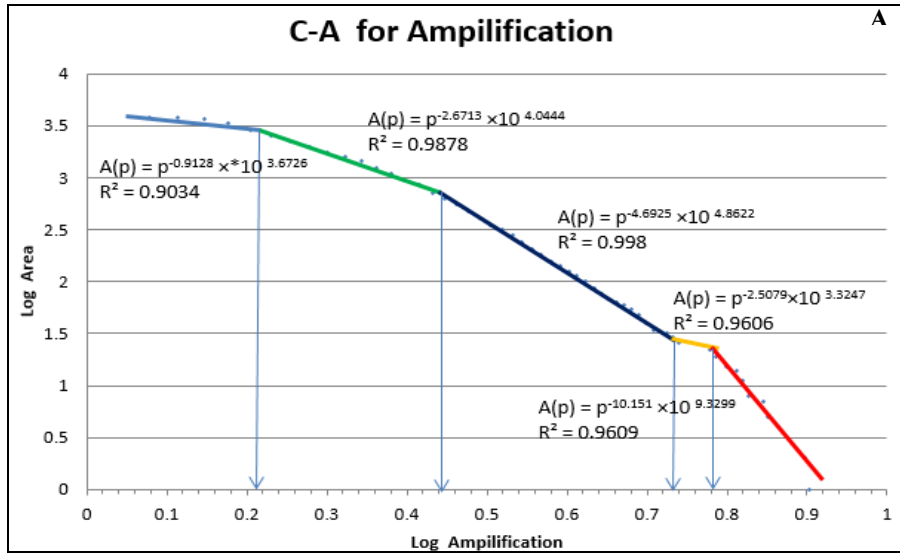
4

5

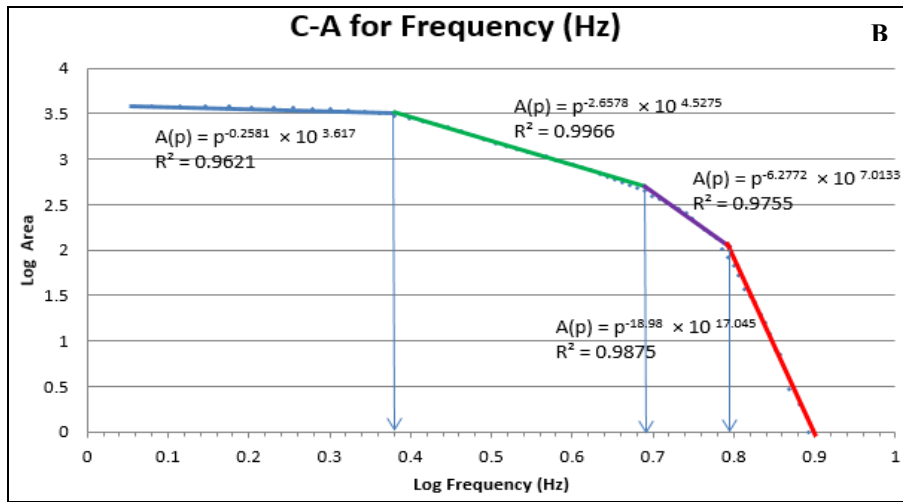
Figure 6. Variograms and anisotropic ellipsoids of the parameters: A) Frequency; B) amplification; C) K-g value.

6 According to the C-A log-log plots, four populations were distinguished for the frequency and
 7 five populations for the amplification and K-g which reveals multifractal nature for the
 8 parameters in the Meybod city, as depicted in Fig 7. There are multifractal nature for
 9 frequency, amplification and K-g based on the more than two straight segments. The straight
 10 segments fitted lines were derived based on least-square regression (Spalla et al., 2010). All
 11 R-squared values are higher than 0.9 and most of them have R^2 higher than 0.95 which is
 12 show a proper straight line fitting for the populations (Fig. 7). The power-law relationships
 13 between the geophysical parameters and their occupied areas were indicated in the Fig. 7.
 14 According to the Eq. 2, there is different values for α which is exponent equal to fractal
 15 dimensions, as depicted in Fig. 7. The variation of fractal dimensions reveals a multifractal
 16 nature for frequency, amplification and K-g in the area. Moreover, a sudden exchanges shows
 17 different populations in the log-log plots especially in the last population (Fig. 7). Data
 18 distribution based on C-A model has been shown in Fig 8. The sites with high intensity values
 19 of frequency are situated in the central parts of the area and the sites with high intensive
 20 amplification and K-g are located in the northern and eastern parts of the Meybod city.

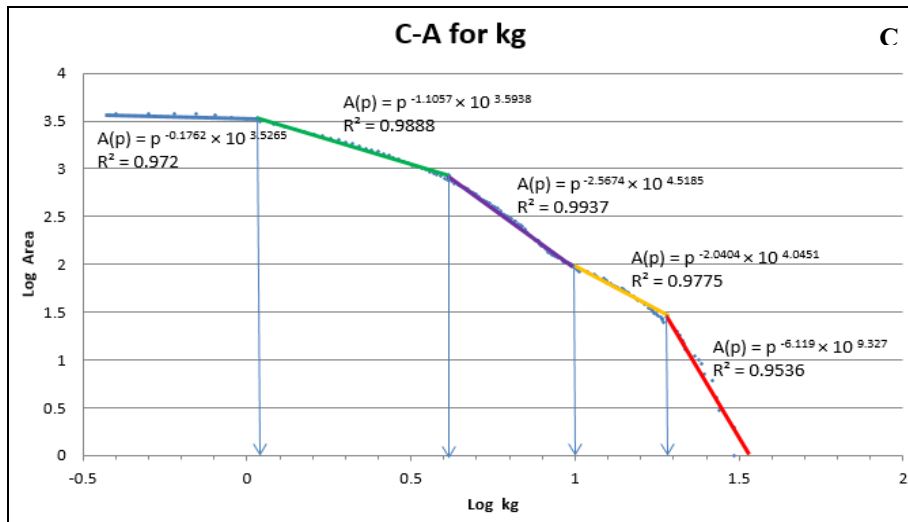
1



2



3

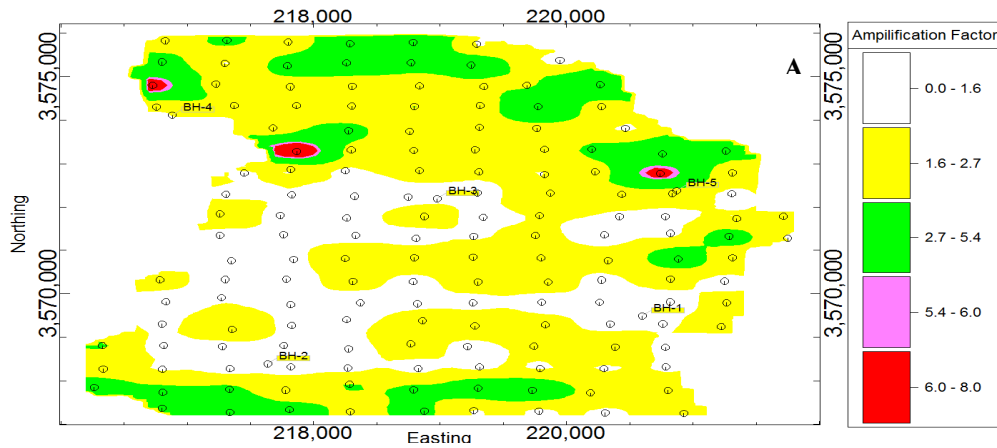


4

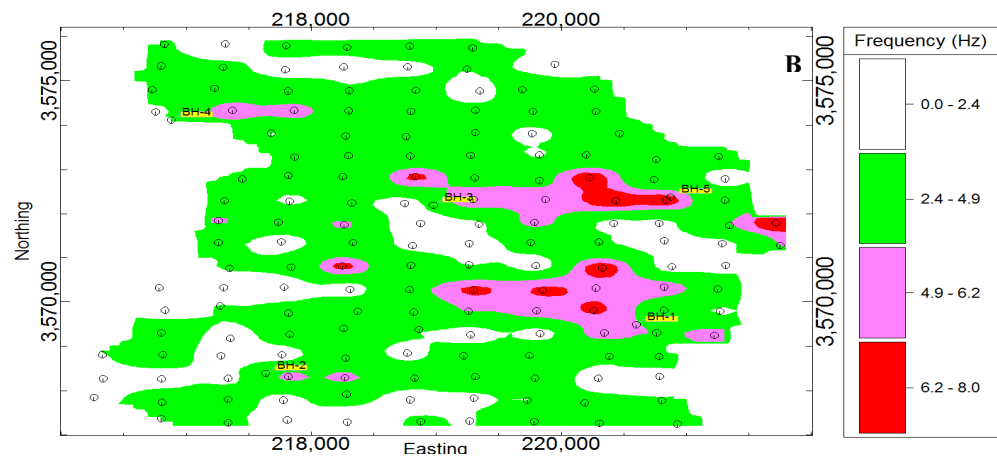
5 Figure 7. C-A log-log plot for the parameters: A) frequency, B) amplification, C) K-g value.

1 The most part of the city has frequency lower than 4.9 Hz, especially between 2.4 to 4.9 Hz.
 2 The central part of the city is the only part with high frequency, as depicted in Fig 8. It
 3 represents that it is more competent than the other parts. Based on the resulted frequencies,
 4 the most parts of the city contain soft soils, but amplification and K-g quantities are very low,
 5 lower than 2.4 and 4.2, respectively.

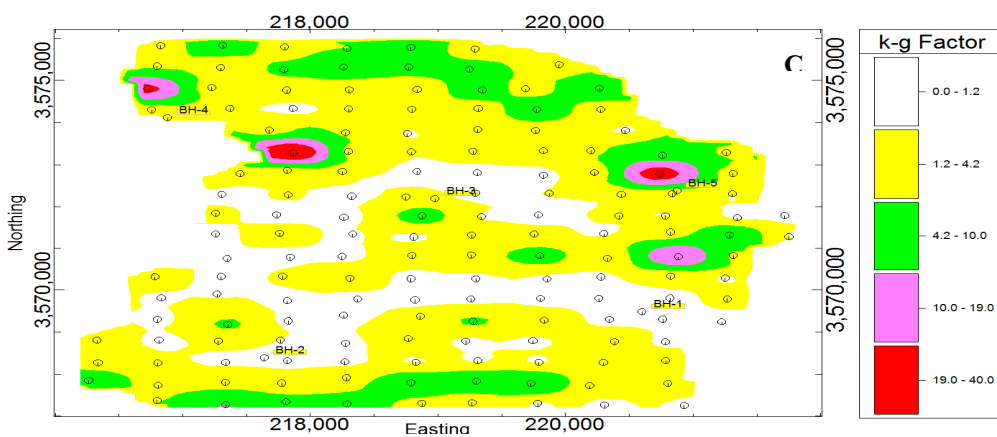
6



7



8



9 Figure 8. Data classification based on C-A method. A) frequency, B) amplification, C) K-g

10 value.

1 **5 Comparison between Nogoshi classification and Fractal modeling results**

2 Site classification of the city is calculated based on Nogoshi and Igarashi method (1970;
3 1971) which is a common classification for microtremor analysis. The basis of this
4 classification is fundamental frequency, thus, with regard to the obtained frequencies, ground
5 type of Meybod is achieved that it has shown in Table 3 and Fig 9.

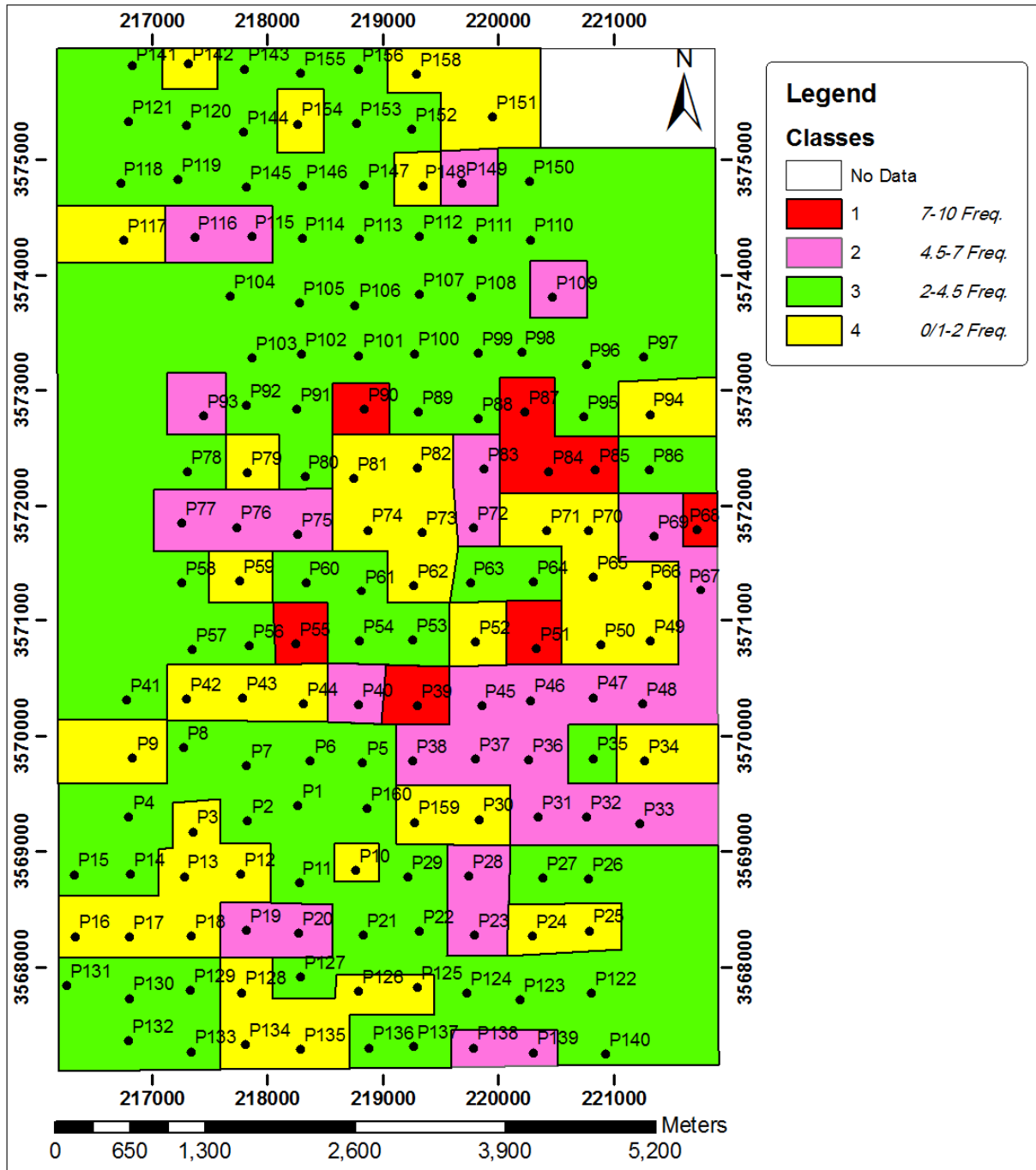


Figure 9. Ground type zonation of the region based on Nogoshi & Igarashi (1970, 71).

1 Comparison between the C-A fractal model and Nogoshi classification shows that the
 2 thresholds obtained by the both methods are similar (Table 4). Indeed it can be said that by
 3 frequency separation resulted from fractal C-A model, we can identify data minor anomalies
 4 and consequently classify site effect results more accurately. Therefore, by this approach
 5 other results due to frequency, can be classified and then every category attributed to one
 6 specific ground type.

7 Table 4. Comparison of frequency separation by C-A fractal model and Nogoshi & Igarashi
 8 (1970, 1971).

Nogoshi		C-A fractal model	
Frequency (Hz)	Ground type	Frequency (Hz)	Category
7-10	I	6.2-8	4
4.5-7	II	4.9-6.2	3
2-4.5	III	2.4-4.9	2
0.1-2	IV	0-2.4	1

9

10 By comparing the soil zonation maps, it is obvious that there are five categories for
 11 amplification and K-g value. Meanwhile, there are four categories due to frequency and
 12 ground classification. Generally, the amplification of the city is low because of very low
 13 variation in the soil composition. Based on the amplification and K-g values (Table 5) of
 14 every frequency category, appropriate quantities of amplification and vulnerability index in
 15 any resulted classes of the C-A fractal model were derived (Table 6). Accordingly,
 16 amplification and k-g in any frequency category are respectively: lower than 2.7 and lower
 17 than 1.2 for frequency between 6.2-8 Hz, lower than 5.4 and lower than 4.2 for frequency 4.9-
 18 6.2 and lower than or equal to 10 and 40 for the other both frequency groups.

19 Based on the results obtained by shear wave velocity calculation in the boreholes and results
 20 derived via the C-A fractal model, the velocities were correlated with threshold values of the
 21 C-A model (Table 3).

22

23

1 Table 5. Frequency of amplification and K-g classes in every frequency category

Frequency Classes (Hz)	Amplification Classes					K-g Classes				
	<1.6	1.6-2.7	2.7-5.4	5.4-6	6-10	<1.2	1.2-4.2	4.2-10	10-19	19-40
6.2-8	4	10	0	0	0	14	0	0	0	0
4.9-6.2	15	5	2	0	0	19	3	0	0	0
2.4-4.9	22	21	12	2	2	28	25	3	1	2
<2.4	28	18	18	0	1	20	24	16	3	2

2

3 Table 6. Site effect classification based on C-A method

Site description	Frequency (Hz)	Amplification	K-g
hard soil, weak rock	6.2-8	<2.7	<1.2
stiff soil	4.9-6.2	<5.4	<4.2
moderately soft soil	2.4-4.9	<10	≤40
soft soil	0-2.4	<10	≤40

4

5 **6 Conclusions**

6 The C-A fractal model is a useful approach in geophysical analysis to identify anomalies and
 7 geological particulars and this has been proved by numerous studies. Also this method could
 8 be appropriate for geophysical distribution analysis due to its fractal nature.

9 In this study, due to comparing site effect classification of the area based on Nogoshi and
 10 Igarashi classification and frequency categorization resulted from the C-A fractal model, it is
 11 obtained that the C-A fractal model is a useful tool to distinguish and classify site effect
 12 results, so that category boundaries could be recognized more accurately. Therefore, the
 13 results are presented better and more suitable and also we can attribute resulted frequency,
 14 amplification and vulnerability index to any site class more confidently. Additionally, the

1 thresholds derived via Nogoshi and Igarashi classification for the region were corrected.
2 Accordingly, four site classes were obtained for the city as follows:
3 - Category 1 (weak rock, hard soil): Frequency between 6.2-8 Hz, amplification lower than
4 2.7 and vulnerability index lower than 1.2. It exists in some points of the center of the city
5 toward the east.
6 - Category 2 (stiff soil): Frequency between 4.9-6.2 Hz, amplification lower than 5.4 and
7 vulnerability index lower than 4.2. It exists mostly in the central parts of the city.
8 - Category 3 (moderately soft soil): Frequency between 2.4-4.9 Hz, amplification lower than
9 10 and vulnerability index lower than or equal to 40. It exists in the most parts of the city.
10 - Category 4 (soft soil): Frequency lower than 2.4 Hz, amplification lower than 10 and
11 vulnerability index lower than or equal to 40, similar to category 3. It is scattered in the
12 different parts of the city such as east and SE, west and SW, center and NW of the area.

13

14 **Acknowledgementsome**

15 The authors thank Islamic Azad University -South Tehran branch for support of this research.
16 In addition, the authors acknowledge Dr. Gholamreza shoei (assistant professor at
17 engineering geology group, geology section, Tarbiat Modares University) and Mr. Alireza
18 Ashofteh for their remarkable contribution.

19

20 **References**

21 Afzal, P., Zia Zarifi, A., Yasrebi, A. B., 2012. Identification of uranium targets based on
22 airborne radiometric data analysis by using multifractal modeling, Tark and Avanligh
23 1:50000 sheets, NW Iran. *Journal of Nonlinear Processes in Geophysics*, 19, 283-289.
24 Afzal, P., Khakzad, A., Moarefvand, P., Rashidnejad Omran, N., Efsan-diari, B., Fadakar
25 Alghalandis, Y., 2010. Geochemical anomaly separation by multifractal modeling in Kahang
26 (Gor Gor) porphyry system, Central Iran. *Journal of Geochemical Exploration* 104, 34-46.
27 Agterberg, F.P., Cheng, Q., Brown, A., Good, D., 1996. Multifractal modeling of fractures in
28 the Lac du Bonnet batholith, Manitoba. *Comput. Geosci.* 22 (5), 497-507.

- 1 Akamatu, K., 1961. On microseisms in frequency range from 1 c/s to 200 c/s. Bull.
2 Earthquake Res. Inst., 39: 23-75.
- 3 Allam, A. M., 1969. An Investigation Into the Nature of Microtremors Through Experimental
4 Studies of Seismic Waves. University of Tokyo, 326 p.
- 5 Architectural Institute of Japan, 1993. Earthquake Motion and Ground Condition. AIJ, AIJ, 5-
6 26-20 Shiba, Minato-ku, Tokyo 108, *Japan*
- 7 Bard, P. Y., 1998. Microtremor measurements: a tool for site effects estimation? Proceedings
8 of the Second International Symposium on the effects of Surface Geology on Seismic Motion,
9 Yokohama, Japan, December 1998, 1251–1279, 1998TS5.
- 10 Bard, P.Y., 2000. Lecture notes on ‘Seismology, Seismic Hazard Assessment and Risk
11 Mitigation’. International Training Course, Potsdam, p. 160
- 12 Beroya, M.A.A., Aydin, A., Tiglao, R., Lasala, M., 2009. Use of microtremor in liquefaction
13 hazard mapping. *Engineering Geology* 107, 140-153.
- 14 Bolviken, B., Stokke, P.R., Feder, J., Jossang, T., 1992. The fractal nature of geochemical
15 landscapes. *J. Geochem. Explor.* 43, 91–109.
- 16 Cheng, Q., Agterberg, F.P., Ballantyne, S.B., 1994. The separation of geochemical anomalies
17 from background by fractal methods. *J. Geochem. Explor.* 51, 109–130.
- 18 Cheng, Q., 1999. Spatial and scaling modelling for geochemical anomaly separation. *J.*
19 *Geochem. Explor.* 65 (3), 175–194.
- 20 Cheng, Q., 2007. Mapping singularities with stream sediment geochemical data for prediction
21 of undiscovered mineral deposits in Gejiu, Yunnan Province, China. *Ore Geol. Rev.* 32, 314–
22 324.
- 23 Daneshvar Saein, L., Rasa, I., Rashidnejad Omran, N., Moarefvand, P., and P. Afzal, 2012.
24 Application of concentration-volume fractal method in induced polarization and resistivity
25 data interpretation for Cu-Mo porphyry deposits exploration, case study: Nowchun Cu-Mo
26 deposit, SE Iran. *Nonlinear Processes in Geophysics.*, 19, 431–438.
- 27 Davis, J.C., 2002. *Statistics and data analysis in Geology* (3th ed.). John Wiley & Sons Inc.,
28 New York, p. 638.

- 1 Douze E.J., 1964. Rayleigh waves in short period seismic noise. *Bull. Seism. Soc. Am.*, Vol.
2 54, 1197-1212.
- 3 Duval, A.M., 1994. Détermination de la réponse d'un site aux séismes à l'aide du bruit de
4 fond: Évaluation expérimentale. PhD Thesis. Université Pierre et Marie Curie, Paris 6. in
5 French.
- 6 Duval, A. M., 1996. Détermination de la réponse d'un site aux séismes à l'aide du bruit de
7 fond, Evaluation expérimentale, Etudes et Recherches des Laboratoires des Ponts et
8 Chaussées, Série Géotechnique. ISSN 1157-39106, 264 pp., Paris : Laboratoire central des
9 ponts et chaussées, ISBN 2-7208-2480 -1, in French, 264 pp.
- 10 Evertz, C.J.G., Mandelbrot, B.B., 1992. Multifractal measures (appendix B). In: Peitgen, H.-
11 O., Jurgens, H., Saupe, D. (Eds.). *Chaos and Fractals*, Springer, New York, p. 953.
- 12 Gettings, M.E., 2005. Multifractal magnetic susceptibility distribution models of
13 hydrothermally altered rocks in the Needle Creek Igneous Center of the Absaroka Mountains,
14 Wyoming. *Nonlinear Processes in Geophysics* 12, 587-601.
- 15 Goncalves, M.A., 2001. Characterization of geochemical distributions using multifractal
16 models. *Math. Geol* 33 (1), 41-61.
- 17 Goncalves, M.A., Mateus, A., Oliveira, V., 2001. Geochemical anomaly separation by
18 multifractal modeling. *J. Geochem. Explor.* 72, 91-114.
- 19 Gosar, A., Stoper, R., Roser, J., 2008. Comparative test of active and passive multichannel
20 analysis of surface waves (MASW) methods and microtremor HVSR method. *RMZ Material
21 and Geo-environment* 55 (1), 41-66.
- 22 Gosar, A., Roser, J., 2010. Microtremor study of site effects and soil-structure resonance in
23 the city of Ljubljana (central Slovenia). *Bulletin of Earthquake Engineering* 8, 571-592.
- 24 Guest, B., Axen, G. J., Lam, P. S. and Hassanzadeh, J., 2006. Late Cenozoic shortening in the
25 west-central Alborz Mountains, northern Iran. *Geosphere*, 2, 35-52.
- 26 Halsey, T.C., Jensen, M.H., Kadanoff, L.P., Procaccia, I., Shraiman, B.I., 1986. Fractal
27 measures and their singularities: the characterization of strange sets. *Phys. Rev. A* 33 (2),
28 1141-1151.

- 1 Heidari, S.M., Ghaderi, M. and Afzal, P., 2013. Delineating mineralized phases based on
2 lithochemical data using multifractal model in Touzlar epithermal Au-Ag (Cu) deposit,
3 NW Iran. *Applied Geochemistry* 31, 119-132.
- 4 Kamalian, M., Jafari, M.K., Ghayamghamian, M.R., Shafiee, A., Hamzehloo, H.,
5 Haghshenas, E., Sohrabi-bidar, A., 2008. Site effect microzonation of Qom, Iran. *Engineering*
6 *Geology* 97, 63-79
- 7 Kanai, K., Tanaka, T., 1954. Measurement of the microtremor I. *Bulletin of the Earthquake*
8 *Research Institute* 32, 199-209.
- 9 Komak Panah, A., Hafezi Moghaddas, N., Ghayamghamian, M. R., Motosaka, M., Jafari, M.
10 K., and Uromieh, A., 2002. Site Effect Classification in East-Central of Iran. *Journal of*
11 *Seismology and Earthquake Engineering*, Vol.4, No.1, pp. 37-46,
- 12 Konno, K and Ohmachi, T., 1998. ground motion characteristics estimated from spectral ratio
13 between horizontal and vertical components of microtremor. *Bulletin of the Seismological*
14 *Society of America*, 88, 228–241.
- 15 Lima, A., De Vivo, B., Cicchella, D., Cortini, M., Albanese, S., 2003. Multifractal IDW
16 interpolation and fractal filtering method in environmental studies: an application on regional
17 stream sediments of (Italy), Campania region. *Applied Geochemistry* 18, 1853–1865.
- 18 Mandelbrot, B.B., 1983. *The Fractal Geometry of Nature*. W. H. Freeman, San Fransisco, p.
19 468.
- 20 Mukhopadhyay, S., Bormann, P., 2004. Low cost seismic microzonation using microtremor
21 data: an example from Delhi, India. *Journal of Asian Earth Sciences* 24, 271-280.
- 22 Nakamura, Y., 1989. A method for dynamic characteristics estimation of subsurface using
23 microtremor on the ground surface, *Quarterly report of Railway Technical Res. Inst. (RTRI)*,
24 30:1, 25-33.
- 25 Nakamura, Y., 1996. Real-time information systems for hazard mitigation. *Proceedings of the*
26 *10th World Conference in Earthquake Engineering*, Anchorage, Alaska, Paper # 2134.
- 27 Nogoshi, M. and T. Igarashi, 1971. On the amplitude characteristics of microtremor (Part 2).
28 *Jour. seism. Soc. Japan*, 24, 26-40 (in Japanese with English abstract).

- 1 Nogoshi, M. and T. Igarashi, 1970. On the propagation characteristics of microtremors.
2 Journal of the Seismological Society of Japan 23, 264-280.
- 3 SESAME, European research project WP12: 2004. Guidelines for the implementation of
4 the H/V spectral ratio technique on ambient vibrations: measurements, processing and
5 interpretation. Available at: http://sesame-fp5.obs.ujf-grenoble.fr/Delivrables/Del-D23-HV_User_Guidelines.pdf.
6 Last accessed July 2011.
- 7 Sim, B.L., Agterberg, F.P., Beaudry, C., 1999. Determining the cutoff between background
8 and relative base metal contamination levels using multifractal methods. Comput. Geosci. 25,
9 1023–1041.
- 10 Spalla, M.I., Morotta, A.M., Gosso, G., 2010. Advances in interpretation of geological
11 processes: refinement of multi-scale data and integration in numerical modelling. Geological
12 Society, London, 240 p.
- 13 Turcotte, D.L., 1986. A fractal approach to the relationship between ore grade and tonnage.
14 Econ. Geol. 18, 1525–1532.
- 15 Turcotte, D.L., 1997. Fractals and Chaos in Geology and Geophysics. Cambridge University
16 Press, Cambridge.
- 17 Xie, S., Cheng, Q., Zhang, S., Huang, K., 2010. Assessing microstructures of pyrrhotites in
18 basalts by multifractal analysis. Nonlinear Processes in Geophysics 17, 319-327.